Family of tunable spherically symmetric potentials that span the range from hard spheres to waterlike behavior

Zhenyu Yan,[1] Sergey V. Buldyrev,[2,1] Nicolas Giovambattista,[3] Pablo G. Debenedetti,[3] and H. Eugene Stanley[1]
[1]*Center for Polymer Studies and Department of Physics, Boston University, Boston, Massachusetts 02215, USA*
[2]*Department of Physics, Yeshiva University, 500 West 185th Street, New York, New York 10033, USA*
[3]*Department of Chemical Engineering, Princeton University, Princeton, New Jersey 08544-5263, USA*
(Received 24 January 2006; published 17 May 2006)

We investigate the equation of state, diffusion coefficient, and structural order of a family of spherically symmetric potentials consisting of a hard core and a linear repulsive ramp. This generic potential has two characteristic length scales: the hard and soft core diameters. The family of potentials is generated by varying their ratio, λ. We find negative thermal expansion (thermodynamic anomaly) and an increase of the diffusion coefficient upon isothermal compression (dynamic anomaly) for $0 \leqslant \lambda < 6/7$. As in water, the regions where these anomalies occur are nested domes in the (T,ρ) or (T,P) planes, with the thermodynamic anomaly dome contained entirely within the dynamic anomaly dome. We calculate translational and orientational order parameters (t and Q_6), and project equilibrium state points onto the (t,Q_6) plane, or order map. The order map evolves from waterlike behavior to hard-sphere-like behavior upon varying λ between 4/7 and 6/7. Thus, we traverse the range of liquid behavior encompassed by hard spheres ($\lambda=1$) and waterlike ($\lambda \sim 4/7$) with a family of tunable spherically symmetric potentials by simply varying the ratio of hard to soft-core diameters. Although dynamic and thermodynamic anomalies occur almost across the entire range $0 \leqslant \lambda \leqslant 1$, waterlike structural anomalies (i.e., decrease in both t and Q_6 upon compression and strictly correlated t and Q_6 in the anomalous region) occur only around $\lambda=4/7$. Waterlike anomalies in structure, dynamics and thermodynamics arise solely due to the existence of two length scales, with their ratio λ being the single control parameter, orientation-dependent interactions being absent by design.

DOI: 10.1103/PhysRevE.73.051204 PACS number(s): 61.20.−p, 05.20.Jj

I. INTRODUCTION

Most liquids become denser when cooled and more viscous when compressed. In contrast, water becomes less dense when cooled (density, or thermodynamic, anomaly) and its diffusivity increases upon compression (diffusion, or dynamic, anomaly). These anomalies, which disappear at high enough temperature and pressure, are not unique to water. Other liquids with local tetrahedral order (e.g., silica and silicon) also exhibit thermodynamic and dynamic anomalies [1]. A possible explanation of these anomalies is the tendency of these substances to form local open structures not present in simple liquids. However, establishing a precise and quantitative link between the microscopic structure and the dynamic and thermodynamic anomalies of tetrahedral liquids has proved elusive until recently.

Errington and Debenedetti [2] (ED) studied the relation between microscopic structure and the anomalies of liquid water by introducing two simple metrics: a translational order parameter t [3], quantifying the tendency of molecule pairs to adopt preferential separations, and an orientational order parameter q [2,4], quantifying the extent to which a molecule and its four nearest neighbors adopt a tetrahedral local structure, as in the case of hexagonal ice. A useful way of investigating structural order in liquids is to map state points into the $t-q$ plane. Such a representation was introduced by Torquato and co-workers [5], who first applied it to sphere packings and referred to it as an order map. ED used the order map to investigate structural order in water [2]. Because of the distinctive features discovered in that study, in what follows we refer to water-like order maps as the ED order map. Using molecular dynamics simulation of the SPC/E [6] model, ED found that the state points accessible to liquid water define a two-dimensional region in the $t-q$ plane, meaning that in general t and q are independently variable in liquid water (i.e., equilibrium state paths exist along which one order metric varies while the other does not). They also found a dome-shaped region in the (T,ρ) plane within which isothermal compression leads to a decrease in t and q. This *decrease* in order upon compression constitutes a structural anomaly: simple liquids, in contrast, always become more ordered upon compression. ED further found that dynamic and thermodynamic anomalies define nested domes in the (T,ρ) plane: the structural anomalies dome contains the dynamic anomalies dome, which in turn contains the thermodynamic anomalies dome. This means that whenever the thermal expansion coefficient is negative, the diffusivity must necessarily increase upon isothermal compression. ED showed that all state points exhibiting structural, dynamic or thermodynamic anomalies define a line on the (t,q) plane, meaning that when water exhibits anomalous behavior, its translational and orientational order metrics become strictly coupled. This is clear evidence of the relationship between structure and water anomalies. Shell, Debenedetti, and Panagiotopoulos subsequently found qualitatively similar behavior in molten silica's order map [7]. However, in the case of silica, it was found that state points corresponding to anomalous behavior define a narrow stripe in the (t,q) plane instead of a strict line. Furthermore, unlike in water, the region of dynamic anomalies was found to contain that of structural anomalies.

For simple spherically symmetric liquids, including hard spheres [5,8] and Lennard-Jones [3], the order map was found to be a positively sloped line in the (t,q) plane, indicating that translational and orientational order are always strictly and positively correlated. In this case, of course, the appropriate metric for orientational order does not measure tetrahedrality; rather, the bond-orientational order parameter introduced by Steinhardt, Nelson, and Ronchetti [9] was used. An important result from these studies is the fact that the order map for the Lennard-Jones system above its critical density is identical to that of hard spheres. Furthermore, in these simple systems that do not exhibit thermodynamic or dynamic anomalies, compression always leads to an increase in the order metrics.

In 1970 Hemmer and Stell [10] showed that in fluids interacting via pairwise-additive, spherically symmetric potentials consisting of a hard core plus an attractive tail, softening of the repulsive core can produce additional phase transitions. This pioneering study elicited a considerable body of work on so-called core-softened potentials [10–18]. This generic term denotes continuous potentials with inflections in the repulsive core [11], discontinuous potentials with the core softened by shoulders or ramps [10,12,14–17], or lattice models with nearest-neighbor-attraction and next-nearest-neighbor repulsion [18]. It is now well established that such potentials can generate waterlike density and diffusion anomalies [10–18]. This important finding implies that strong orientational interactions, such as those that exist in water and silica, are not a necessary condition for a liquid to have thermodynamic and dynamic anomalies.

The above discussion implies the existence of two well-defined classes of liquids: simple and waterlike. The former, which interact via spherically symmetric nonsoftened potentials, do not exhibit thermodynamic nor dynamic anomalies, and their order map is a line. In waterlike liquids, interactions are orientation-dependent; these liquids exhibit dynamic and thermodynamic anomalies, and their order map is, in general, two-dimensional but becomes linear (or quasi-linear) when the liquid exhibits structural, dynamic or thermodynamic anomalies. Intermediate between these well-defined extremes is the class of core-softened liquids, which interact via spherically-symmetric potentials but can also exhibit water-like thermodynamic and dynamic anomalies.

Two questions arise naturally from this emerging taxonomy of liquid behavior. First, is structural order in core-softened fluids hard sphere or waterlike? Second, is it possible to seamlessly connect the range of liquid behavior from hard spheres to waterlike by a simple and common potential, simply by changing a physical parameter?

In a recent study [19] we addressed the first question. We showed that a core-softened potential with two characteristic length scales not only can give rise to waterlike diffusive and density anomalies, but also to an ED waterlike order map. This implies that orientational interactions are not necessary in order for a liquid to have structural anomalies. In this work we address the second question. Specifically, we use the ratio of characteristic length scales as a control parameter to investigate the evolution of dynamic, thermodynamic and structural anomalies. In this manner we show that the family of tunable spherically symmetric potentials so generated evolves continuously between waterlike and hard sphere behavior.

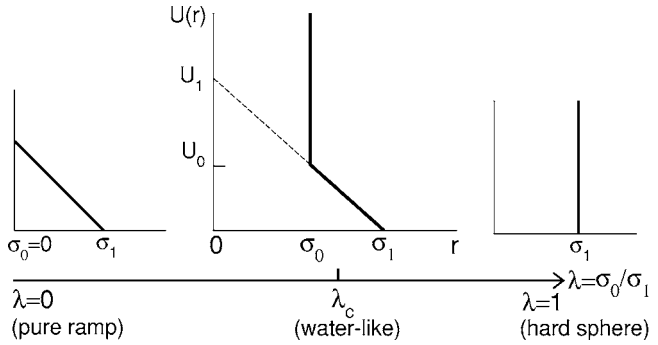

FIG. 1. The middle figure shows the ramp potential with two characteristic length scales; σ_0 corresponds to the hard core, σ_1 characterizes the onset of soft repulsion. When $\lambda=0$ (left figure) we have a pure ramp potential (no hard core). When $\lambda=1$ (right figure) we have a hard sphere potential. $\lambda_c \sim 0.6$ is the ratio near which the system exhibits waterlike structural, dynamic and thermodynamic behavior.

This paper is structured as follows. Secs. II–IV provide details on the interaction potential, simulation method, and order parameters, respectively. Results are presented in Sec. V. Conclusions and some suggestions for future work are provided in Sec. VI.

II. RAMP POTENTIAL

We perform discrete molecular dynamics (MD) simulations to study the equation of state, diffusion coefficient and structural order as measured by the ED order map, for a fluid whose particles interact via a pairwise-additive, spherically symmetric potential that gives rise to both thermodynamic and dynamic waterlike anomalies. The model was introduced by Jagla [12]; the potential energy $U(r)$ between a pair of particles separated by a distance r is given by (see Fig. 1)

$$U(r) = \begin{cases} \infty & r < \sigma_0 \\ U_1(\sigma_1 - r)/\sigma_1 & \sigma_0 \leqslant r \leqslant \sigma_1 \\ 0 & r > \sigma_1 \end{cases} . \tag{1}$$

The shorter distance σ_0 corresponds to the hard core, and the longer distance σ_1 characterizes a softer repulsion range that can be overcome at high pressure. Because of its shape, it is called the ramp potential. The constant slope of the ramp potential for $\sigma_0 < r < \sigma_1$ keeps the force between particles f constant, so the product of separation and force rf will decrease when the separation r decreases. This satisfies the mathematical meaning of core-softening [18] and under these conditions the thermodynamic (density) anomaly can be qualitatively explained by invoking the virial theorem [18].

Of interest is the ratio between the two characteristic length scales, σ_0 and σ_1

$$\lambda \equiv \sigma_0/\sigma_1, \tag{2}$$

which can vary between 0 and 1. Reference [19] investigated the one-scale ($\lambda=0$) and two-scale ($\lambda=4/7$) ramp potentials.

Here we investigate the full range $0<\lambda<1$, with $\lambda=0,2/7,4/7,5/7,6/7$.

III. MD SIMULATION

We use discrete MD simulation; details are given in Ref. [17]. We use the NVT ensemble (i.e., the number of particles N, the volume V, and the temperature T of the system are kept constant) for a system composed of 850 particles with periodic boundary conditions, and we control the temperature with the Berendsen thermostat [20]. However, we note that we use different units than in Ref. [17]: the distance r, number density ρ, pressure P and temperature T are all normalized with respect to the soft core distance σ_1 and the potential U_1 at $r=0$ (i.e., densities are reported as $\rho\sigma_1^3$, and temperature as kT/U_1). We also investigate systems with different number of particles ($N=1728$) and confirm that the results do not depend on the number of particles. The simulation ranges of temperature and density fully cover the region where density, diffusion and structural anomalies occur.

The location of freezing lines for soft potentials requires special attention [21]. We verify that the systems we have studied are in the liquid phase by applying the technique described in Ref. [17], in which the ramp potential's phase diagram is investigated for $\lambda=4/7$, including both the melting and homogeneous nucleation lines. In the supercooled state, the system can be equilibrated for a sufficiently long time, and quantities such as the pressure and the potential energy fluctuate without drift about average values that can be computed with high accuracy. As soon as nucleation occurs, the potential energy decreases sharply, and the pressure experiences periodic jumps because of finite system size and the use of periodic boundary conditions. When such an event occurs we disregard the data obtained after nucleation. Moreover, it has been shown for the hard-sphere [5,8] and Lennard-Jones systems [3], that the structural order parameters jump discontinuously when the system crystallizes. In our system we observe only continuous changes in the order parameters, which clearly indicates that the system is in the liquid state.

IV. TRANSLATIONAL AND ORIENTATIONAL ORDER PARAMETERS

A. Translational order parameter

The translational order parameter [2,3,7] is defined as

$$t \equiv \int_0^{s_c} |g(s)-1|ds. \tag{3}$$

Here $s\equiv r\rho^{1/3}$ is the radial distance r scaled by the mean interparticle distance $\rho^{-1/3}$, ρ is the number density, $g(s)$ is the pair correlation function, and s_c a numerical cutoff. We choose s_c so that it corresponds to one-half the simulation box size, and we verify that our system size is always large enough so that $g(s)=1$ at half the box size. For a completely uncorrelated system, $g(s)\equiv 1$, and thus $t=0$. For systems with long-range order, the modulations in $g(s)$ persist over large distances, causing t to grow. Between these limits, t will change as a consequence of the dependence of $g(r)$ upon T and ρ.

B. Orientational order parameter

An orientational order parameter based on spherical harmonic function was introduced by Steinhardt, Nelson, and Ronchetti [9] and used in Refs. [3,5,8,22]. In this definition, all vectors connecting nearest neighbors (i.e., particle pairs whose separation is less than the first minimum of the radial distribution function) are considered. Each of these vectors, also called "bond," defines an azimuthal and polar angle, and the corresponding spherical harmonic function is evaluated. The orientational order parameter used in Refs. [3,5,8,22] involves the average of each spherical harmonic function over all bonds.

The orientational order parameter used for water and silica in Refs. [2,7] involves, first, the evaluation of the local tetrahedral order for each particle with respect to its four nearest neighbors, and then, the average of this quantity over all the molecules of the system. In the definition of the orientational order parameter used in Refs. [3,5,8,22] there is no such concept of "local order" for an individual particle. Moreover, the number of bonds associated with each particle is not fixed, but instead it changes with temperature and pressure. These two differences led, in Ref. [19], to the introduction of a slightly modified version of the original orientational order parameter introduced by Steinhardt and coworkers in Ref. [9]. The resulting order metric is based on the idea of a local order for each particle, analogous to Refs. [2,7]. The ED maps obtained with the original (global) and modified (local) definitions of orientational order are qualitatively similar.

In this work we use the same order parameter introduced in Ref. [19]. We define 12 bonds connecting each particle to its 12 nearest neighbors. Each bond is characterized by its azimuthal and polar angles (θ,φ) and the corresponding spherical harmonic $Y_{\ell m}(\theta,\varphi)$ is computed. The orientational order parameter associated with each particle i is

$$Q_{\ell i} \equiv \left[\frac{4\pi}{2\ell+1}\sum_{m=-\ell}^{m=\ell}|\bar{Y}_{\ell m}|^2\right]^{1/2}. \tag{4}$$

Here, $\bar{Y}_{\ell m}(\theta,\varphi)$ denotes the average of $Y_{\ell m}(\theta,\varphi)$ over the 12 bonds associated with particle i. For $\ell=6$ [3], $Q_{\ell i}$ has a large value for most crystals such as fcc, hcp and bcc [9]. The values of Q_{6i} for each molecule in the system follow a Gaussian distribution. Q_6, the averaged value of Q_{6i} over all particles i, is used to characterize the local order of the system. This definition of order parameter is analogous to that used in water. For water, the solid at low pressure is hexagonal ice where each molecule has four neighbors. The orientational order parameter is maximum in the ice configuration and decreases as the system becomes less icelike. For the ramp potential, the solid phase at low pressure has an fcc structure where each particle has 12 nearest neighbors. Q_6 has a maximum value in the fcc lattice ($Q_6^{\mathrm{fcc}}=0.574$) and decreases as the system becomes less correlated (for uncorrelated systems, $Q_6=1/\sqrt{12}=0.289$).

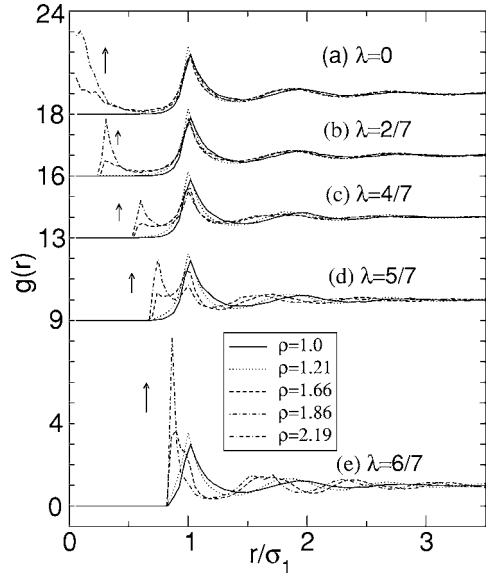

FIG. 2. Radial distribution function $g(r)$ at $T=0.04$ for different $\lambda \equiv \sigma_0/\sigma_1$ values. The arrows indicate the direction of increasing density. The density values are 1.0, 1.21, 1.66, 2.19 for $\lambda=2/7,4/7,5/7$ and 1.0, 1.21, 1.66, 1.86 for $\lambda=0,6/7$. The distance r is normalized by σ_1, the soft core length. The curves for different λ are shifted vertically by integer numbers for clarity.

V. RESULTS AND DISCUSSION

A. Structural anomalies and order map

Since the pair correlation function $g(r)$ is used to compute the translational order parameter t [Eq. (3)], we first discuss the effect of density on $g(r)$. Figure 2 shows the effects of compression on $g(r)$ at low temperature, $T=0.04$, for the various values of λ considered in this study. In all cases, there is no inner peak at $r=\sigma_0$ for $\rho=1$ and 1.21, and only the outer peak at $r=\sigma_1$ is present at these densities. The inner peak at $r=\sigma_0$, which is broad and of modest height at $\rho=1.66$, becomes sharper and more pronounced upon further compression. Interestingly, structural changes brought about by compression become progressively longer ranged as λ increases. Thus, for $\lambda=0$ and 2/7, the major changes in $g(r)$ involve the development of structure at length scales $\leqslant\sigma_1$ associated with the growth of the inner peak at $r=\sigma_0$. However, for $\lambda=4/7$, 5/7 and 6/7, structural changes upon compression also occur at distances larger than σ_1. In particular, for $\lambda=6/7$, the effects of compression are clearly discernible at $r=3\sigma_1$.

These effects of density on the pair correlation function underlie the evolution of t upon compression, shown in Figs. 3(a1)–3(e1). Consider, for example, the $T=0.04$ isotherm when $\lambda=2/7$. It can be seen that t displays a nonmonotonic dependence on density: it increases upon compression at low densities, $1.0<\rho<1.22$, decreases over the intermediate density range $1.22<\rho<1.76$, and increases again at high densities, $\rho>1.76$. The initial increase at low densities is associated with the growth of $g(\sigma_1)$. The emergence of structure associated with the inner (hard) core causes t to decrease at intermediate densities because the initial, modest growth of g at $r\sim\sigma_0$ causes $|g-1|$ to decrease with respect to its low-density value of 1 [see Eq. (3)]. Upon further compression, the growth of $g(\sigma_0)$ above 1 eventually contributes additional area to the integral of $|g-1|$, causing t to increase. This qualitative behavior of t is similar for $\lambda=0$, 2/7 and 4/7, and is more pronounced at low T. For $\lambda=6/7$, close to the hard sphere limit, the pronounced growth of the inner peak upon compression gives rise to a monotonic density dependence of t, and structural changes upon compression occurring at distances larger than σ_1 have less effect since g converges to 1 by $r/\sigma_1\sim3$. The case $\lambda=5/7$ is clearly transitional, with nonmonotonic behavior at low temperature changing to hard-sphere-like monotonic growth of t upon compression at high temperature.

Orientational order, as measured by Q_6, shows a pronounced dependence on λ, illustrated in Figs. 3(a2)–3(e2). When $\lambda=0$ (no hard core), Q_6 increases monotonically with density for all T. When $\lambda=2/7$, Q_6 begins to exhibit nonmonotonic behavior upon compression. For this particular

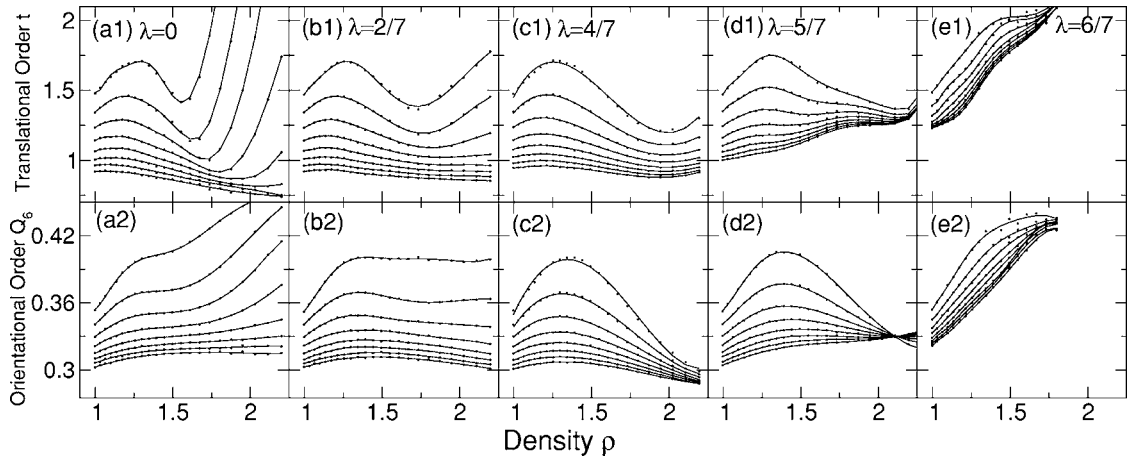

FIG. 3. The upper and lower panels (a1)-(e1) and (a2)-(e2) show the density dependence of the translational order parameter t and orientational order parameter Q_6 for $\lambda=0$ (a1, a2), 2/7 (b1, b2), 4/7 (c1, c2), 5/7 (d1, d2), and 6/7 (e1, e2). The solid lines are polynomial fits to the data. In each panel, the different curves correspond to isotherms (top to bottom) $T=0.03,0.04,0.05,0.06,0.07,0.08,0.09,0.10$.

value of λ the trend is very mild, and is best described as a virtual insensitivity of Q_6 to compression, except for an initial increase at low enough densities. For λ=4/7 and 5/7, orientational order exhibits a marked nonmonotonic dependence on density, especially at low temperatures. When coupled with the corresponding behavior of t, this corresponds to a waterlike structural anomaly, whereby both order metrics decrease upon isothermal compression. When λ =6/7, which is close to the hard sphere value (λ=1), orientational order increases monotonically upon compression. Thus, there exists a narrow interval of λ within which the ramp fluid shows waterlike structural order, whereas in the pure ramp (λ=0) and quasi-hard-sphere limits (λ∼1) Q_6 behaves conventionally upon compression. The fact that t displays strongly nonmonotonic behavior for λ=0 and 2/7, while Q_6 only shows very mild nonmonotonic behavior at λ=2/7 illustrates the much weaker coupling of the two order metrics compared to the waterlike case (λ=4/7).

Cross plotting the order metrics against each other generates the order map, whose evolution as a function of λ is depicted in Fig. 4. For all values of λ except 6/7, state points fall on a two-dimensional region, signifying that t and Q_6 can be varied independently. As is the case for silica and water [2,7], we find, for all values of λ, an inaccessible region where no liquid state points can be found. In the pure ramp (λ=0) case, the pronounced nonmonotonic dependence of t on density gives rise to isotherms with well-characterized t minima, the locus of which defines the boundary between the accessible and inaccessible regions of the order map. For λ=2/7, the barely discernible nonmonotonic dependence of Q_6 on density gives rise to loops along isotherms. The nonmonotonic behavior of Q_6 is fully developed for λ=4/7. This gives rise to an order map with states corresponding to structural anomalies lying on a narrow stripe of the order map adjacent to the boundary between the accessible and inaccessible regions. This behavior is strikingly analogous to that of water. The insensitivity of structural order to temperature, a distinguishing feature of hard spheres, can be clearly seen in Fig. 4(e) by the virtual collapse of all isotherms in the λ=6/7 case. The transition from waterlike to hard sphere order map occurs in the narrow interval $4/7<\lambda<6/7$. In particular, for λ=5/7, there is a clear evolution from waterlike low-T behavior ($T<0.07$) to hard-sphere-like high-T behavior ($T>0.07$).

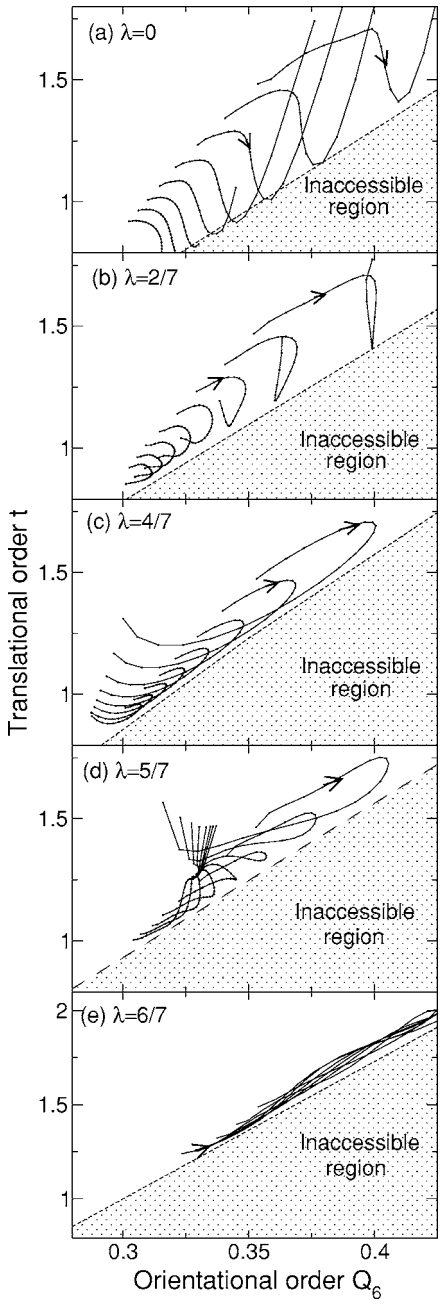

FIG. 4. Order map of the ramp fluid for different λ. For each λ, the eight isotherms (right to left) correspond to $T=0.03,0.04,0.05,0.06,0.07,0.08,0.09,0.10$, and the arrow indicates the direction of increasing density.

B. Thermodynamic, dynamic, and structural anomalies

We now discuss the regions of the phase diagram where structural, dynamic and thermodynamic anomalies occur. In water [2], structural, dynamic, and thermodynamic anomalies occur as nested domes in the (T,ρ) or (T,P) planes. Structural anomalies define the outer dome, within which isothermal compression results in a decrease of both translational and orientational order. Dynamic anomalies define an intermediate dome, lying entirely within the structural anomalies dome, and within which isothermal compression leads to an increase in the diffusion coefficient. Thermodynamic anomalies define the innermost dome, within which water expands when cooled isobarically. In silica [7], dynamic anomalies define the outer dome, structural anomalies the intermediate dome, and thermodynamic anomalies define the inner dome. Thus, in both cases negative thermal expansion also implies diffusive and structural anomalies, but in silica diffusive anomalies occur over a broader range of densities and temperatures than structural anomalies, the opposite being true in water.

Figure 5 shows the loci of dynamic and thermodynamic anomalies for three values of λ. The latter line was traced by locating extrema of isochores in the (P,T) plane. Similar to water and silica, in ramp fluids thermodynamic anomalies

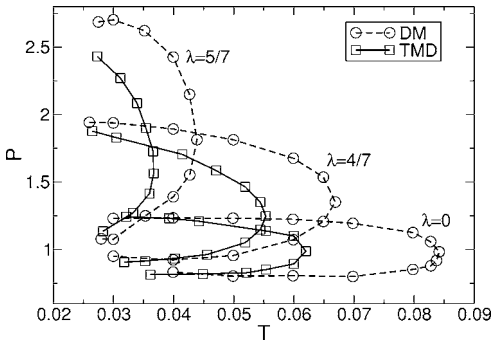

FIG. 5. Loci of thermodynamic and dynamic anomalies for ramp fluids with different λ values. The region of diffusion anomalies is defined by the loci of diffusion minima and maxima (DM) inside which the diffusivity increases upon isothermal compression. The thermodynamically anomalous region is defined by the locus of temperatures of maximum density (TMD), inside of which the density increases when the system is heated at constant pressure.

occur over a narrower temperature and density range than dynamic anomalies. In other words, if a ramp fluid is at a state point where it expands when cooled isobarically, its diffusion coefficient necessarily increases upon isothermal compression. It can be seen that upon increasing λ, the range of temperatures where anomalies occur shrinks, and there are no anomalies for $\lambda=6/7$, whereas the upper limit of density (or pressure) where anomalies can occur increases. The shrinking of the temperature range where anomalies occur follows from the fact that increasing λ makes the fluid progressively hard-sphere-like, and there are no anomalies in a hard sphere fluid.

Figure 6 shows the relationship between the loci of dynamic, thermodynamic and structural anomalies. In water, the low-density and high-density branches of the dome of structural anomalies correspond to tetrahedrality maxima and translational order minima, respectively. For the pure ramp case ($\lambda=0$), the orientational order increases monotonically with density over the range of temperatures explored here. Accordingly, as seen in Fig. 6(a), the dynamic and thermodynamic anomalies domes are bounded by loci of translational order extrema (maxima: line C; minima: line A). Between lines C and A, compression leads to a decrease in translational order. For $\lambda=4/7$ and $5/7$, the locus of orientational order maxima (B) provides a low-density bound to the existence of thermodynamic and dynamic anomalies. Thus, for these two values of λ, ramp fluids exhibit a waterlike cascade of anomalies (structural, dynamic, thermodynamic). For $\lambda=2/7$, Q_6 maxima are barely discernible and the two order metrics are only weakly coupled to each other. Accordingly, the locus of weak orientational order maxima (B) is not a relevant indicator of dynamic or thermodynamic anomalies.

VI. CONCLUSION

In this work we have investigated thermodynamic, dynamic and structural anomalies in ramp potential fluids, as a function of the ratio λ of length scales corresponding to the inner hard core, and to the outer edge of the ramp. We find that thermodynamic and dynamic anomalies exist for $\lambda=0$, $2/7$, $4/7$ and $5/7$, but not for $=6/7$. As in water and silica, the loci of anomalies form nested domes in the (T,ρ) plane, inside which the thermal expansion coefficient is negative (inner dome) and the diffusivity increases upon compression (outer dome). The limit $\lambda=1$ corresponds to hard spheres, and the absence of anomalies for $\lambda=6/7$ indicates approach to hard sphere behavior. The order map of this family of ramp fluids is waterlike at $\lambda=4/7$ and hard-sphere-like at $\lambda=6/7$. Thus, by varying the ratio of characteristic length scales, the family of ramp potentials spans the range of liquid behavior from hard spheres to waterlike.

These findings show that orientational interactions are not necessary for the existence of thermodynamic, dynamic, or structural anomalies. Instead, waterlike behavior apparently emerges in this spherically symmetric family of fluids through the existence of two competing length scales, with their ratio λ being the single control parameter. Although thermodynamic and dynamic anomalies exist almost over the entire range of the control parameter, the combination of thermodynamic and dynamic anomalies plus a water-like or-

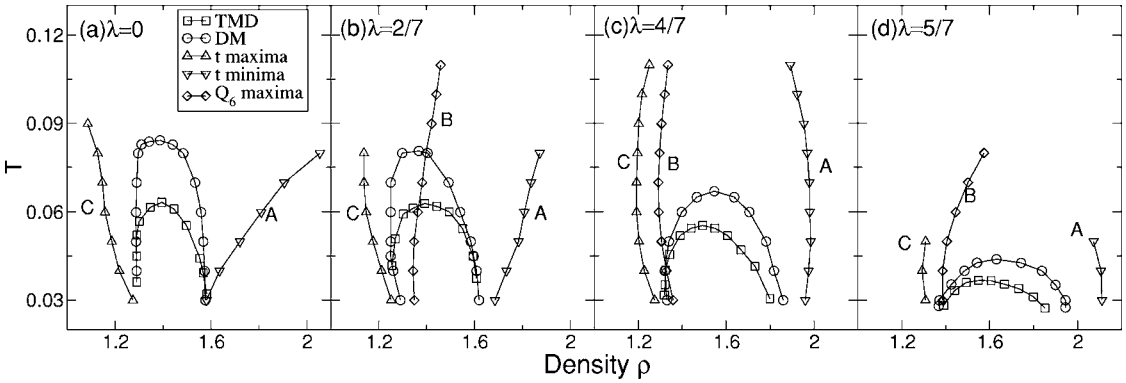

FIG. 6. Relationship between structural order and the density and diffusion anomalies in the $\rho-T$ plane. For $\lambda=0$ and $2/7$, the domes of dynamic and thermodynamic anomalies are bounded by loci of *t* maxima (C) and minima (A), between which isothermal compression causes a *decrease* in translational order. For $\lambda=4/7$ and $5/7$, the domes of dynamic and thermodynamic anomalies are bounded by loci of Q_6 maxima (B) and *t* minima (A), between which isothermal compression causes a *decrease* in both translational and orientational order (structural anomaly). This cascade of anomalies is characteristic of water.

der map occurs over a narrow range of λ. It is interesting to note that a distinguishing feature of water is the fact that the ratio of radial distances to the first and second peaks of the oxygen-oxygen pair correlation function is not $\sim 1/2$, as in simple liquids, but ~ 0.6. This is close to 0.571 ($\lambda = 4/7$, the ratio of σ_0 to σ_1 that gives rise to waterlike structural, dynamic and thermodynamic anomalies). In water, isothermal compression pushes molecules from the second shell towards the first shell, gradually filling the interstitial space [23]. Likewise, in the ramp potential, isothermal compression pushes molecules from the soft core (σ_1) to the hard core (σ_0). Further work is needed to establish whether a ratio of competing length scales close to 0.6 is generally associated with waterlike anomalies in other core-softened potentials, for example, linear combinations of Gaussian [24] potentials. In this work we used the terminology waterlike to denote structural, diffusion, and density anomalies. The increase in water's isothermal compressibility upon isobaric cooling, another of this liquid's canonical anomalies, is also trivially captured by the ramp potential, because thermodynamic consistency arguments [25] mandate that the compressibility increases upon cooling whenever there exists a negatively sloped locus of density maxima in the (P,T) plane.

The ramp potential, when supplemented by explicit [13,26] or mean-field attractions [12], gives rise to liquid-liquid immiscibility and a critical point distinct from the one associated with the vapor-liquid transition. A liquid-liquid transition has been observed experimentally in phosphorus [27,28], n-butanol [29] and triphenyl phosphite [30], and strong experimental evidence consistent with liquid-liquid immiscibility also exists for water [31–33]. Computer simulations of silicon [34], silica [35], carbon [36] and water [37–43] also indicate the presence of a liquid-liquid transition. A systematic study of the effects of λ and the ratio of characteristic energies (U_1 and the attractive well depth) on the existence of a liquid-liquid transition, the positive or negative slope of the line of first-order liquid-liquid transitions in the (P,T) plane, and the relationship, if any [16], between the liquid-liquid transition and density anomalies, would shed important new light on the phenomenon of liquid polyamorphism [1,44,45].

It is generally accepted that strong orientation-dependent interactions underlie many of the distinctive properties of associating, network-forming liquids such as water. Atomic liquids, on the other hand, exhibit simpler behavior, and in particular do not show structural, thermodynamic, or dynamic anomalies of the type discussed here. In this work we have shown that key properties of these apparently distinct categories of liquids can be bridged systematically by varying the ratio of two length scales in a family of spherically symmetric potentials in which orientation-dependent interactions are absent by design. What other spherically symmetric potentials, in addition to those possessing competing length scales, may give rise to waterlike anomalies, is among the interesting questions arising from this study that we will pursue in future work.

ACKNOWLEDGMENTS

We thank NSF Grant Nos. CHE 0096892 and CHE 0404699 for support and Yeshiva University for CPU time.

[1] C. A. Angell, R. D. Bressel, M. Hemmatti, E. J. Sare, and J. C. Tucker, Phys. Chem. Chem. Phys. **2**, 1559 (2000).
[2] J. R. Errington and P. G. Debenedetti, Nature (London) **409**, 318 (2001).
[3] J. R. Errington, P. G. Debenedetti, and S. Torquato, J. Chem. Phys. **118**, 2256 (2003).
[4] P. L. Chau and A. J. Hardwick, Mol. Phys. **93**, 511 (1998).
[5] S. Torquato, T. M. Truskett, and P. G. Debenedetti, Phys. Rev. Lett. **84**, 2064 (2000).
[6] H. J. C. Berendsen, R. J. Grigera, and T. P. Stroatsma, J. Phys. Chem. **91**, 6269 (1987).
[7] M. S. Shell, P. G. Debenedetti, and A. Z. Panagiotopoulos, Phys. Rev. E **66**, 011202 (2002).
[8] T. M. Truskett, S. Torquato, and P. G. Debenedetti, Phys. Rev. E **62**, 993 (2000).
[9] P. J. Steinhardt, D. R. Nelson, and M. Ronchetti, Phys. Rev. B **28**, 784 (1983).
[10] P. C. Hemmer and G. Stell, Phys. Rev. Lett. **24**, 1284 (1970); G. Stell and P. C. Hemmer, J. Chem. Phys. **56**, 4274 (1972); J. M. Kincaid, G. Stell, and C. K. Hall, *ibid.* **65**, 2161 (1976); J. M. Kincaid, G. Stell, and E. Goldmark, *ibid.* **65**, 2172 (1976); J. M. Kincaid and G. Stell, *ibid.* **67**, 420 (1977).
[11] F. H. Stillinger and D. K. Stillinger, Physica A **244**, 358 (1997).
[12] E. A. Jagla, J. Chem. Phys. **111**, 8980 (1999);
[13] E. A. Jagla, Phys. Rev. E **63**, 061509 (2001).
[14] M. R. Sadr-Lahijany, A. Scala, S. V. Buldyrev, and H. E. Stanley, Phys. Rev. Lett. **81**, 4895 (1998); Phys. Rev. E **60**, 6714 (1999).
[15] A. Scala, M. R. Sadr-Lahijany, N. Giovambattista, S. V. Buldyrev, and H. E. Stanley, J. Stat. Phys. **100**, 97 (2000); Phys. Rev. E **63**, 041202 (2001).
[16] G. Franzese, G. Malescio, A. Skibinsky, S. V. Buldyrev, and H. E. Stanley, Nature (London) **409**, 692 (2001); Phys. Rev. E **66**, 051206 (2002).
[17] P. Kumar, S. V. Buldyrev, F. Sciortino, E. Zaccarelli, and H. E. Stanley, Phys. Rev. E **72**, 021501 (2005).
[18] P. G. Debenedetti, V. S. Raghavan, and S. S. Borick, J. Phys. Chem. **95**, 4540 (1991).
[19] Z. Yan, S. V. Buldyrev, N. Giovambattista, and H. E. Stanley, Phys. Rev. Lett. **95**, 130604 (2005).
[20] M. P. Allen and D. J. Tildesley, *Computer Simulation of Liquids* (Clarendon, Oxford, 1990).
[21] C. N. Likos, A. Lang, M. Watzlawek, and H. Lowen, Phys. Rev. E **63**, 031206 (2001).
[22] A. Huerta, G. G. Naumid, D. T. Wasan, D. J. Henderson, and A. D. Trokhymchuk, J. Chem. Phys. **120**, 1506 (2004).
[23] F. Sciortino, A. Geiger, and H. E. Stanley, J. Chem. Phys. **96**, 3857 (1992).
[24] F. F. Stillinger, J. Chem. Phys. **65**, 3968 (1976).

[25] S. Sastry, P. G. Debenedetti, F. Sciortino, and H. E. Stanley, Phys. Rev. E **53**, 6144 (1996).
[26] L. Xu, P. Kumar, S. V. Buldyrev, S.-H. Chen, P. H. Poole, F. Sciortino, and H. E. Stanley, Proc. Natl. Acad. Sci. U.S.A. **102**, 16558 (2005).
[27] Y. Katayama, T. Mizutani, W. Utsumi, O. Shimomura, M. Yamakata, and K. Funakoshi, Nature (London) **403**, 170 (2000).
[28] Y. Katayama, Y. Inamura, T. Mizutani, M. Yamakata, W. Utsumi, and O. Shimomura, Science **306**, 848 (2004).
[29] R. Kurita and H. Tanaka, J. Phys.: Condens. Matter **17**, L293 (2005).
[30] R. Kurita and H. Tanaka, Science **306**, 845 (2004).
[31] O. Mishima and H. E. Stanley, Nature (London) **392**, 164 (1998).
[32] O. Mishima, Phys. Rev. Lett. **85**, 334 (2000).
[33] O. Mishima and Y. Suzuki, Nature (London) **419**, 599 (2002).
[34] S. Sastry and C. A. Angell, Nat. Mater. **2**, 739 (2003).
[35] I. Saika-Voivod, F. Sciortino, and P. H. Poole, Phys. Rev. E **63**, 011202 (2001).
[36] J. N. Glosli and F. H. Ree, Phys. Rev. Lett. **82**, 4659 (1999).
[37] P. H. Poole, F. Sciortino, U. Essmann, and H. E. Stanley, Nature (London) **360**, 324 (1992).
[38] S. Harrington, R. Zhang, P. H. Poole, F. Sciortino, and H. E. Stanley, Phys. Rev. Lett. **78**, 2409 (1997).
[39] M. Yamada, H. E. Stanley, and F. Sciortino, Phys. Rev. E **67**, 010202(R) (2003).
[40] P. H. Poole, I. Saika-Voivod, and F. Sciortino, J. Phys.: Condens. Matter **17**, L431 (2005).
[41] M. Yamada, S. Mossa, H. E. Stanley, and F. Sciortino, Phys. Rev. Lett. **88**, 195701 (2002).
[42] I. Brovchenko, A. Geiger, and A. Oleinikova, J. Chem. Phys. **118**, 9473 (2003).
[43] I. Brovchenko, A. Geiger, and A. Oleinikova, J. Chem. Phys. **123**, 044515 (2005).
[44] P. H. Poole, T. Grande, C. A. Angell, and P. F. McMillan, Science **275**, 322 (1997).
[45] J. L. Yarger and G. H. Wolf, Science **306**, 820 (2004).